Construction and Building Materials 261 (2020) 119971

Contents lists available at ScienceDirect

Construction and Building Materials

journal homepage: www.elsevier.com/locate/conbuildmat

Case studies of up-cycling of partially crystallized ceramic waste in highly porous glass-ceramics

P. Rabelo Monich [a], A. Rincon Romero [a], E. Rambaldi [b], E. Bernardo [a,*]

[a] Dipartimento di Ingegneria Industriale, Università degli Studi di Padova, Via Marzolo, 9 - 3a5131 Padova, Italy
[b] Centro Ceramico, Via Martelli, 26 - 40138 Bologna, Italy

HIGHLIGHTS

- Valorization of polishing residue or vitrified asbestos-containing waste.
- Glass-ceramic foams by alkali activation, gel-casting and sintering.
- Highly porous materials with high strength-to-density ratio were obtained.
- Reduction of process costs by minimizing additives and processing temperatures.
- Soda-lime glass addition favored densification and control of crystal phases.

ARTICLE INFO

Article history:
Received 10 April 2020
Received in revised form 12 June 2020
Accepted 15 June 2020

Keywords:
Waste valorization
Ceramic foams
Alkali activation
Gel-casting
Sintering

ABSTRACT

Highly porous glass-based materials represent a solution for thermal insulation. However, the manufacturing costs still affect their extensive use. The present investigation proposes savings in the production of foams by use of discarded materials, such as polishing residue or vitrified asbestos-containing waste, minimizing additives and processing temperatures. Aqueous suspensions of powders, mixed with soda-lime glass, underwent progressive gelation due to alkali activation. An extensive foaming was determined by mechanical stirring, with the help of a surfactant. Finally, a firing step yielded foams exhibiting excellent strength-to-density ratios, due to densification and control of crystal phases, both supported by the glass addition.

1. Introduction

As energy consumption required for heating and cooling in buildings contributes extensively to carbon emissions worldwide, efficient, safe and low-cost thermal insulators with low environmental impact are increasingly attractive [1]. Glass foams, generally offering an unique combination of properties (e.g. low density and low thermal conductivity comparing well with those of foamed polymer, accompanied by superior mechanical strength), represent an excellent solution for thermal insulation in buildings, due to their distinctive durability [2]. However, the environmental impact in the production of ceramic insulators may be quite high, due to overall energy consumption and intensive use of raw materials [3].

In the particular case of glass foams, the advantage of reusing recycled glass, in commercial products (Foamglas ®, from Pittsburgh Corning), is counterbalanced by the addition of a secondary glass fraction, from an expensive melting process, in order to incorporate ferric and manganic oxides, acting as oxidizers. These components are useful in providing oxygen, by conversion into ferrous and manganous oxides, in turn reacting with carbon black, used as foaming agent [4]. Oxidizing compounds may be used as additive in mixtures of glass and foaming agent, but they still imply additional costs and complications in the processing [5].

The present investigation proposes alternative strategies for reducing the environmental impact and costs of glass-based foams for thermal insulation. Firstly, the process used in this study minimizes the use of additives, as observed in the production of foams from soda-lime glass [6] as well as from glasses for biomedical applications [7], according to an 'inorganic gel casting' approach.

Abbreviations: C, cofalit (vitrified asbestos-containing waste); PR, porcelain stoneware residue; SLG, soda-lime glass.

* Corresponding author.
E-mail address: enrico.bernardo@unipd.it (E. Bernardo).

https://doi.org/10.1016/j.conbuildmat.2020.119971
0950-0618/

In this process, fine glass powders are cast in aqueous solutions comprising alkaline activators (NaOH and KOH), used at a low molarity (usually between 1 and 2.5 M), in plastic containers. The partial dissolution at the surface of glass particles determines the progressive gelation of the obtained suspensions, according to the formation of binding compounds (such as calcium silicate hydrated and alkali hydrated carbonates) on the same surfaces, usually stimulated by a 'curing' step (0–4 h at 70–80 °C). Before the gelation is complete, the suspensions are easily foamed, with the help of a surfactant, by intensive mechanical stirring directly in the containers. As an alternative, the foamed suspensions may be poured in molds, for the sake of homogeneity. Finally, the setting of suspensions is completed in a drying step (8–24 h at 70–80 °C), followed by demolding and firing. Since the foaming is achieved already at nearly room temperature, the firing causes just the consolidation of powders, by viscous flow sintering, with no 'interference' from any reaction (decomposition or oxidation), involving additives, aimed at gas generation. The evident flexibility, from the decoupling of sintering and foaming, has motivated the extension to many other glasses, beyond those previously cited [8].

A second occasion for cost and energy saving comes from the adoption of waste materials with minimized 'handling', i.e. without any significant preliminary treatment. In particular, we referred to two types of semi-crystalline residues, such as powders from the polishing of porcelain stoneware and plasma-vitrified asbestos-containing waste. The polishing residue consists of fine powders deriving from the cutting and polishing or lapping of porcelain stoneware tiles. It is usually reused as by-products [9] in the ceramic process for industries with a complete cycle but in some cases it is still disposed in landfills [10,11]. New building materials, such as innovative ceramic tiles [11] and geopolymers [12], have been already proposed as alternative to landfilling but, in the frame of Circular Economy, further solutions are undoubtedly welcome.

Vitrified asbestos-containing waste ('Cofalit'), on the other hand, refers to the material obtained after plasma vitrification of asbestos-containing materials, from Inertam-Europlasma (France) [13]. The thermal treatment is effective in destroying the harmful fibrous structure of asbestos, but the produced inert material generally finds only low cost applications, in civil engineering, as aggregate for cement and bituminous binders [13,14]. The applications are conditioned by the crystallization occurring upon uncontrolled (slow) cooling of the liquid waste mixture, when cast in large metallic containers, after plasma processing; a previous investigation, in fact, demonstrated that (completely amorphous) frits from remelted Cofalit could lead to valuable dense and porous sintered glass-ceramics [15]. Remelting, as an additional treatment at high temperature, is evidently not sustainable.

The challenge in extending the above-mentioned process to crystalline residues concerns the reactivity in alkaline solution. Glasses are inherently prone to alkali activation, with formation of different 'gelling' compounds, according to their chemistry. Some glasses, as an example, form highly stable, geopolymer-like gels, as shown by Garcia-Lodeiro et al. [16]. The sensitivity to alkaline activation could be enhanced without any 'conditioning' of the waste (i.e. conversion into glass by remelting and fast cooling), by engineered addition of soda-lime glass. Such approach finds an analogy in recent experiences with waste-derived glass exhibiting an unfavorable balance between sintering and crystallization (i.e. excessively rapid crystallization during sintering, hindering the densification by viscous flow) [17]. The addition, besides improving the hardening of suspensions, also enhanced the viscous flow during sintering and caused transformations in the phase assemblage.

2. Materials and methods

The starting partially crystallized residues were in different conditions. Porcelain stoneware residue (PR) corresponded to powders sampled from a landfill site in Emilia-Romagna (Italy); Cofalit (plasma processed asbestos-containing waste, C), on the contrary, was kindly provided by Inertam-Europlasma (France) [13] in form of coarse fragments, which were reduced into powders by dry ball milling. In both cases, the powders were carefully sieved, in order to keep fractions with a maximum particle size below 75 μm. These fractions were considered alone or in mixed with fine soda-lime glass (SLG) powders (medium particle size of 30 μm), supplied by SASIL SpA (Brusnengo, Biella, Italy). The latter powder actually represented an additional waste, being unacceptable as raw material for the manufacturing of new glass articles, due to ceramic contaminations. The chemical composition of all waste materials applied in this study is reported in Table 1.

Fine powders were cast in NaOH (molarity up to 2.5 M) aqueous solutions and left, under low speed mechanical stirring (400 rpm) – for 3 h -, for partial dissolution. After an intermediate 'curing' step (1–2 h at 20–75 °C), the mixtures were cast in polystyrene molds, added with a surfactant (4 wt% Triton X-100, polyoxyethylene octyl phenyl ether – $C_{14}H_{22}O(C_2H_4O)_n$, n = 9–10, Sigma-Aldrich, Gillingham, UK), and finally subjected to intensive mechanical stirring (2000 rpm). After drying at 40 °C for 48 h, hardened suspensions could be first demolded and then fired at 900 °C, for 1 h (heating rate of 10 °C/min). The details concerning four groups of foams, including solid content, molarity of NaOH solution, curing conditions and amount of soda-lime glass added, are reported in Table 2.

The mineralogical analysis was performed on fine powders by means of X-ray diffraction (XRD) (Bruker D8 Advance, Karlsruhe, Germany), employing CuKα radiation, 0.15418 nm, 40 kV–40 mA, 2θ = 10–70°, step size of 0.02°. The semi-automatic Match!® program package (Crystal Impact GbR, Bonn, Germany), supported by data from Powder Diffraction File (PDF)-2 database (International Centre for Diffraction Data, Newtown Square, PA, USA), was applied for phase identification.

Attenuated total reflectance Fourier-transform infrared spectroscopy (ATR-FTIR) was assessed on an Alpha-P spectrometer (Bruker, Germany). The spectra were recorded in the range of 4000 cm^{-1} to 700 cm^{-1}, with a resolution of 4 cm^{-1} for 32 scans.

The developed foams were cut into cubes of approximately 10 mm × 10 mm × 10 mm. These samples were further applied for morphological and mechanical characterization, as well as for density measurements. The geometric density (ρ_{geom}) was evaluated by considering the mass to volume ratio. Apparent (ρ_{app}) and true (ρ_{true}) density data were measured by using a helium pycnometer (Micromeritics AccuPyc 1330, Norcross, GA), operating on bulk or on finely crushed samples, respectively. The three density values were used to compute the amounts of open and closed porosity, according to the following definitions:

$$\rho_{geom} = \frac{mass}{geometrical\ \ volume} = \frac{m}{GV}$$

$$\rho_{app} = \frac{mass}{apparent\ \ volume} = \frac{m}{GV - VOP}$$

$$\rho_{true} = \frac{mass}{true\ \ volume} = \frac{m}{GV - VOP - VCP}$$

Where VOP and VCP are the volumes of open and closed pores, respectively. Fine powders, from crushed samples, were obviously supposed to be pore-free. Combining the definitions, we obtained:

$$\frac{\rho_{geom}}{\rho_{app}} = \frac{\frac{m}{GV}}{\frac{m}{GV-VOP}} = \frac{GV - VOP}{GV} = 1 - f_{OP}$$

Table 1
Chemical composition of polishing stoneware residue, Cofalit and soda-lime glass (wt %).

Oxide	Polishing stoneware residue [18]	Cofalit [15]	Soda-lime glass [6]
SiO_2	64.1	35.7	71.9
Al_2O_3	16.5	7.4	1.2
CaO	1.4	35.1	7.5
Na_2O	4.4	<0.05	14.3
MgO	4.6	12.6	4.0
Fe_2O_3	0.5	7.0	0.3
K_2O	2.1	0.1	0.4
TiO_2	0.5	1.5	0.1
ZrO_2	1.1		
Others	0.8		
LOI	4.0	0.6	0.3

Table 2
Conditions applied in the production of ceramic foams made with polishing residue (PR) or Cofalit (C).

Sample type	PR0SLG	PR10SLG	C10SLG	C30SLG
Soda-lime glass addition (wt%)	0	10	10	30
Alkaline solution	2.5 M NaOH	1 M NaOH	1 M NaOH	1 M NaOH
Solid content (wt%)	63	63	60	60
Curing (before foaming)	1 h at 75 °C	2 h at 75 °C	2 h at 20 °C	2 h at 20 °C

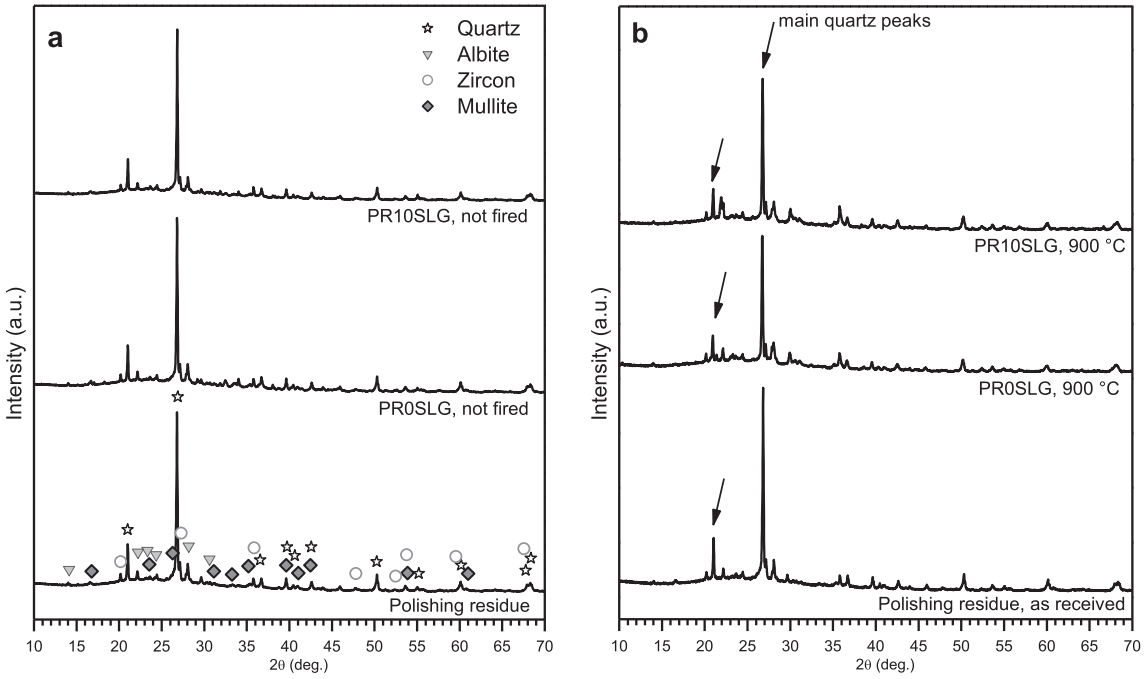

Fig. 1. X-ray diffraction patterns of polishing residue and PR0SLG and PR10SLG: a) after activation; b) after firing.

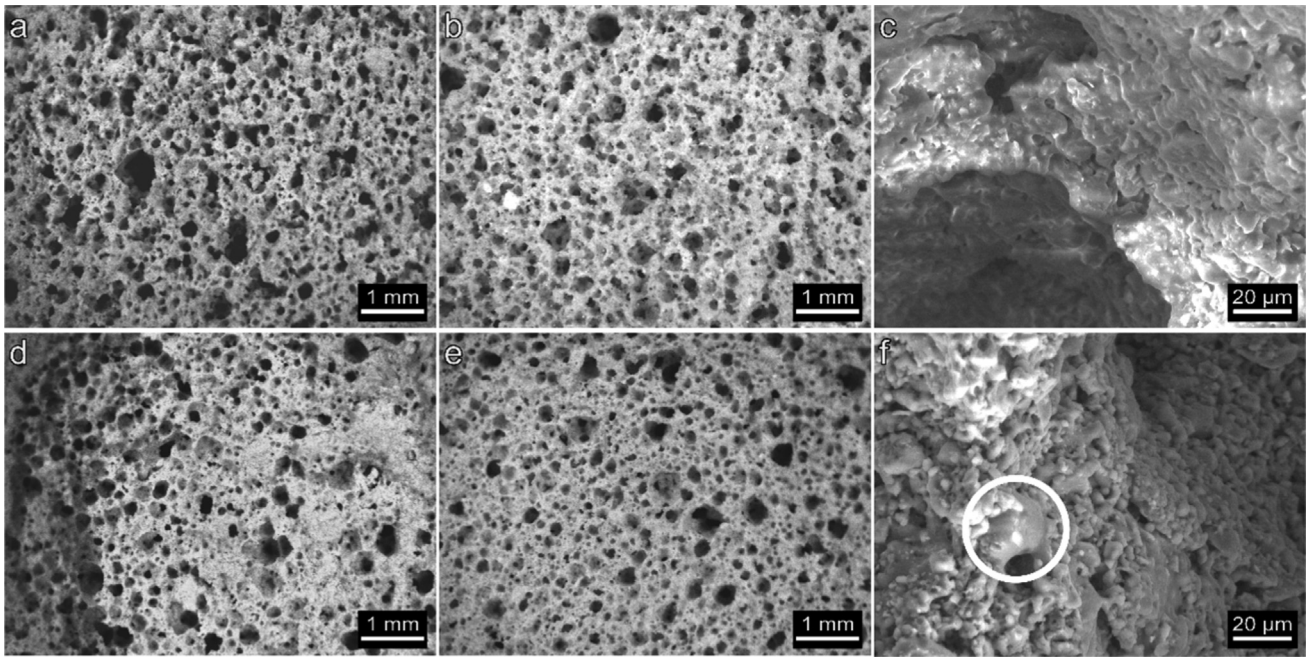

Fig. 2. Polishing stoneware residue-derived foams: a) PR0SLG, 'green' state; b-c) PR0SLG, after firing at 900 °C; d) PR10SLG, 'green' state; e-f) PR10SLG', after firing at 900 °C.

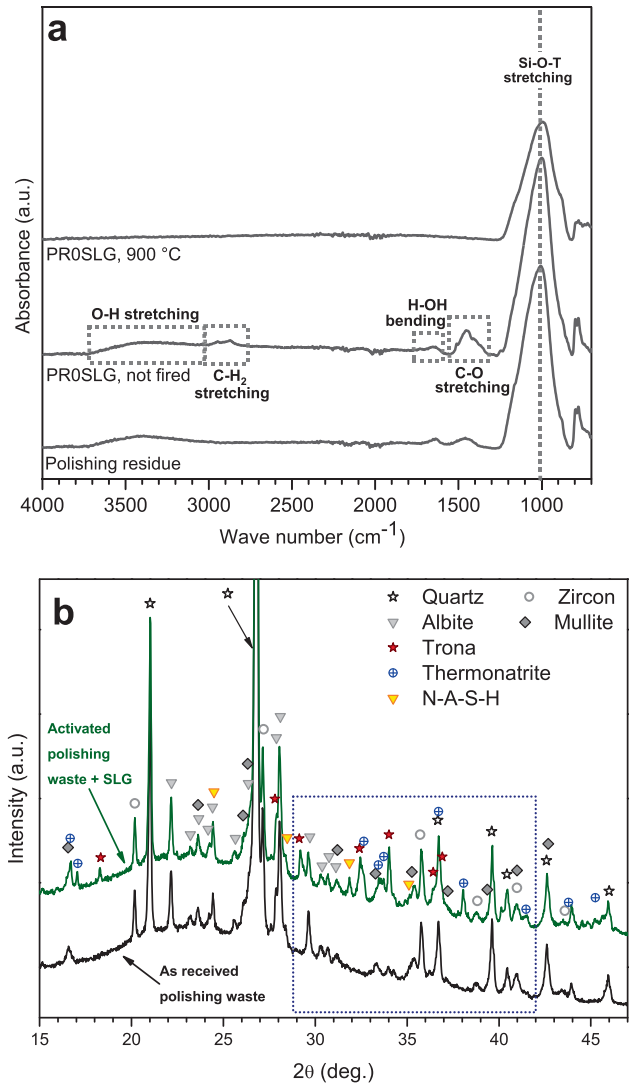

Fig. 3. Activation and transformation of foams from pure polishing waste (samples PR0SLG): a) FTIR spectra; b) X-ray diffraction patterns.

$$\frac{\rho_{geom}}{\rho_{true}} = \frac{\frac{m}{GV}}{\frac{m}{GV-VOP-VCP}} = \frac{GV-VOP-VCP}{GV} = 1 - f_{OP} - f_{CP}$$

The two equations (on density data) yielded the volume fractions of open and closed porosity, f_{OP} and f_{CP}. The determination of open and closed porosity was straightforward (open porosity = f_{OP}·100%; open porosity = f_{CP}·100%).

The morphological and microstructural characterizations of the foams was assessed by using an optical stereomicroscopy (AxioCam ERc 5 s Microscope Camera, Carl Zeiss Microscopy, Thornwood, New York, USA) and a scanning electron microscopy (FEI Quanta 200 ESEM, Eindhoven, The Netherlands).

The compressive strength of fired foams was determined by employing an Instron 1121 UTM (Instron Danvers, MA). The mechanical test was conducted at room temperature with a cross-head speed of 1 mm/min. 7 individual tests were performed for each group of samples.

3. Results and discussion

3.1. Valorization of polishing stoneware residue

The mineralogical analysis of the as received residue, in Fig. 1a, revealed α-quartz (SiO_2, PDF#85-1054) as the main crystalline phase, accompanied by traces of mullite ($3Al_2O_3{\cdot}2SiO_2$, PDF#83-1881), albite (sodium feldspar, $Na_2O{\cdot}Al_2O_3{\cdot}6SiO_2$, PDF#76-0898) and zircon (zirconium silicate, $ZrO_2{\cdot}SiO_2$, PDF#71-0991). This was in good agreement with what known for the phase development in porcelain stoneware: according to Dondi et al. [19], porcelain stoneware tiles typically feature 55–65 wt% of glassy phase, 20–25 wt% of quartz and 12–16 wt% of mullite. In addition, corundum and zircon can also be present in small quantities [19], whereas residual feldspar may be embedded in the glassy matrix [12]. The fact that mullite (from thermal evolution of clay raw materials) could be hardly detected, may indicate that the original porcelain stoneware tile had been fired at quite low temperature [20].

Fig. 2 testifies the effectiveness of the inorganic gel casting process, when applied to porcelain stoneware powders without any additive. Homogeneous 'green' foams were achieved by interaction with a 2.5 M NaOH solution, as shown by Fig. 2a. The cellular structure (consisting of a multitude of nearly spherical pores, with a diameter below 500 μm) was confirmed after firing at 900 °C, as shown by Fig. 2b.

The nature of the gelling compounds was monitored by means of infrared spectroscopy and X-ray diffraction analysis. Fig. 3a shows the infrared spectra of polishing stoneware residue, in the form of as received fine powders as well as powdered foams, before and after firing (group PR0SLG, with no glass addition). It is evident that the alkali activation led to limited transformations, observing the slight variations from the as received conditions. Some bands, being visible after activation but disappearing after firing, can be undoubtedly attributed to newly formed phases, except those at 2800–2900 cm^{-1}, assigned to C-H_2 stretching in the surfactant Triton X-100 [21]. In particular, we could infer the development of hydrated carbonate compounds, from the most clearly distinguishable peak (centered at approximately 1450 cm^{-1}, associated to C-O stretching) and from the slight increase of hydration related band (O–H stretching and H-OH bending bands, at 3000–3500 cm^{-1} and 1650 cm^{-1}, respectively).

No particular difference between the as received and activated condition could be actually inferred by simple mineralogical analysis (Fig. 1a), as done in previous investigations [21,22]. In an attempt to highlight the presence of newly formed phases, we replotted the diffraction signals from as received powders to those from powders after activation in a limited 2θ range, as shown by Fig. 3b. Replotting the patterns very closely yielded a clear evidence of newly formed phase, confirming the results from FTIR analysis, especially in the highlighted 2θ = 29–42° range. In fact, both position and relative intensity of extra peaks, in the pattern from activated material compared to the pattern of as received polishing waste, were consistent with the development of hydrated sodium carbonates, such as thermonatrite ($Na_2CO_3{\cdot}H_2O$, PDF#76-0910) and trona ($Na_3(CO_3)(HCO_3){\cdot}2H_2O$, PDF#89-4125). We could not exclude, in addition, the presence of traces of sodium aluminum silicate hydrate (N-A-S-H, $Na_6(AlSiO_4)_6{\cdot}(H_2O)_8$, PDF#88-1190)

The thermal treatment, despite being applied at much lower temperature than that adopted in the manufacturing of porcelain stoneware tiles (in the order to 1200 °C) [23], led to a good densification of the starting powders, as illustrated by Fig. 2c. The thermal decomposition of Na-containing binding compounds likely caused some alkali intake, in turn enhancing the softening of the glass phase in the particles of polishing residue. Such fluxing action led to some solubilization of quartz, observing the reduced intensity of the relative peaks (marked by arrows) in the mineralogical analysis after firing, in Fig. 1b. No new crystal phase could be detected. It should be noted that the cellular structure in the fired state was mostly conditioned by the low temperature foaming: gas release from the decomposition of both surfactant [6] and hydrated sodium carbonates (trona and thermonatrite) [24] is known to occur at much lower temperature than that adopted in the firing step.

The firing, as reported above, caused a good densification of powders at cell struts, but it did not determine the formation of continuous cell walls. The absence of 'membranes' between adja-

Table 3
Physical and mechanical properties data of fired foams made with polishing stoneware residue or Cofalit.

Group of samples		PR0SLG	PR10SLG	C10SLG	C20SLG	C30SLG
Soda-lime glass addition (wt%)		0	10	10	20	30
Density determinations	ρ_{geom} (g/cm^3)	0.66 ± 0.01	0.64 ± 0.02	0.38 ± 0.01	0.41 ± 0.01	0.57 ± 0.01
	ρ_{app} (g/cm^3)	2.46 ± 0.04	2.59 ± 0.00	3.02 ± 0.01	3.05 ± 0.01	2.98 ± 0.00
	ρ_{true} (g/cm^3)	2.54 ± 0.00	2.59 ± 0.00	3.02 ± 0.01	3.05 ± 0.01	2.98 ± 0.00
Porosity distribution (P)	Total P (vol%)	74.0	75.1	87.3	86.6	80.9
	Open P (vol%)	73.1	75.1	87.3	86.6	80.9
	Closed P (vol%)	0.9	0.0	0.0	0.0	0.0
Strength determinations	σ_{comp} (MPa)	3.1 ± 0.6	2.5 ± 0.4	0.2 ± 0.1	0.5 ± 0.1	2.4 ± 0.2
	σ_{bend} (MPa)	118.7	103.5	20.9	50.6	147.1

cent cells, anyway, did not compromise the achievement of a good strength-to-density ratio, evident from the compressive strength (σ_{comp}), exceeding 3 MPa, coupled with a total porosity of 74% (P = 0.74 = 1-ρ_{rel}, where ρ_{rel} is the 'relative density'), as shown by Table 3. This was confirmed by application of the well-known Gibson and Ashby's model [25,26], ruling the scaling of compressive strength with relative density for open-celled foams, according to the bending strength of the solid phase (σ_{bend}), as follows:

$$\sigma_{comp} = \sigma_{bend} \cdot [0.2(\rho_{rel})^{3/2}]$$

From the experimental data of compressive strength and density we could compute a bending strength exceeding 100 MPa, comparing well with that of dense ceramic tiles made with polishing stoneware residue [11].

The reuse of porcelain stoneware residues in geopolymers is undoubtedly interesting in the perspective of avoiding a firing treatment. We should take into account, however, the higher costs in raw materials and energy, and complications in the overall processing, arising from the adoption of far more aggressive alkaline solutions (highly basic solution of alkali hydroxides and silicates) than that applied in the present case. Since gelation is just an intermediate step, additional savings could be determined by using even 'weaker' alkaline solutions.

With pure polishing residue, a NaOH molarity of 2.5 M actually configured the minimum condition for gelation. Gels developed at lower molarity were all unstable, so that foamed suspensions collapsed already upon drying. A remarkable improvement, however, occurred by introduction of soda-lime glass, already mentioned for its sensitivity to alkaline activation [6]. Fig. 2d, in particular, shows a green foam from a mixture comprising 10 wt% soda-lime glass, keeping the high homogeneity (and pore morphology) of foams from pure porcelain stoneware residue, activated at higher molarity.

The firing at 900 °C consolidated again the structure developed at nearly room temperature, as shown by Fig. 2e. Owing to the reduced amount of activator, we could not expect an intensive fluxing action from the thermal decomposition of the binding phase; however, the additive provided an optimum compensation, as illustrated by Fig. 2f. Particles of polishing residue appear 'glued' by softened soda-lime glass (see the zone marked with a circle; the attribution to soda-lime glass of the matrix was confirmed by energy dispersive X-ray spectroscopy, not shown).

The synergy between porcelain stoneware residue and soda-lime glass was further evidenced by infrared spectroscopy and mineralogical analysis. The activated mixture exhibited bands comparable to those of polishing residue activated alone and at higher molarity (see Fig. 4a); however, the diffraction analysis ('closely packed' patterns in Fig. 4b) revealed a decrease of both thermonatrite and trona, with appearance of sodium aluminum silicate hydrate (N-A-S-H, $Na_6(AlSiO_4)_6 \cdot (H_2O)_8$, PDF#88-1190) and sodium silicate hydrate (revdite, $Na_2Si_2O_5 \cdot 5H_2O$, PDF# 00-033-1279).

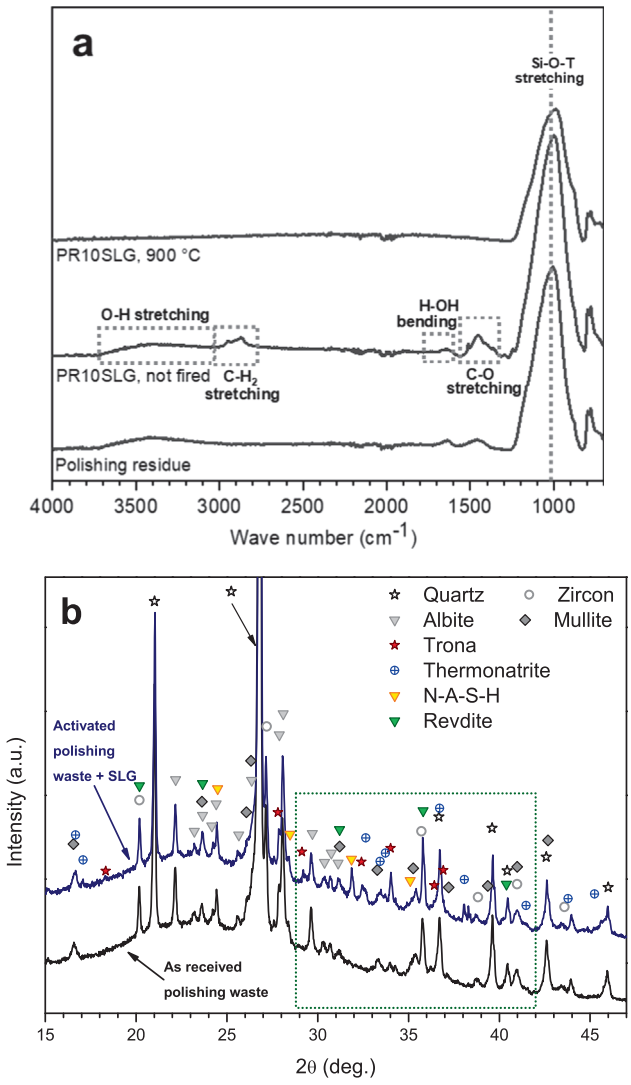

Fig. 4. Activation and transformation of foams from polishing waste mixed with soda-lime glass (samples PR10SLG): a) FTIR spectra; b) X-ray diffraction patterns.

The impact of soda-lime glass, with limited NaOH activator, was analogous to that of higher NaOH content in the solubilization of quartz, upon firing, as shown by Fig. 2b. In addition, Fig. 5 testifies some reduction of the shoulder attributable to mullite traces (2θ ~ 26°), and the appearance of some peaks consistent, in terms of position and relative intensity, with cubic cristobalite (SiO_2, PDF#85-0621). The formation of pure cristobalite is doubtful, since we should consider the possible solubilization of Al^{3+} and Na^+ ions (replacing Si^{4+} ions and positioned in voids, for charge compensation, respectively), forming cristobalite 'stuffed derivatives' (shar-

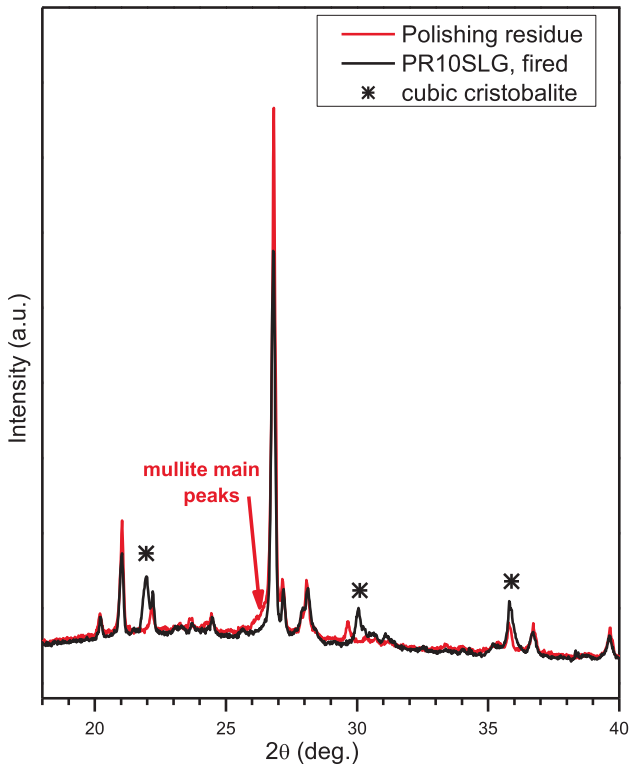

Fig. 5. Detailed mineralogical comparison between as received polishing residue and PRSLG10 foam.

ing the same crystal structure) [27]. In particular, orthorombic carnegieite ($Na_2O{\cdot}Al_2O_3{\cdot}2SiO_2$) is known as the derivative of cubic cristobalite [28].

The strength-to-density ratio, as reported by Table 3, remained quite substantial, with an estimated bending of solid phase still comparing well with that of dense porcelain stoneware and sintered glass-ceramics [18].

3.2. Valorization of Cofalit

The experience on porcelain stoneware residue constituted a reference for the up-cycling of vitrified asbestos-containing waste into highly porous foams. The molarity of the alkaline solution was maintained at low level (1 M NaOH) for several trials. Without glass addition we did not obtain stable gels; on the contrary, a successful foaming and hardening was achieved by mixing the residue from asbestos vitrification with soda-lime glass in an amount from 10 wt% to 30 wt% (see Table 2), as shown by Fig. 6a and d.

The different glass addition did not cause significant changes in the infrared spectra, as shown by Fig. 7 (we report data for 10 and 30 wt% SLG, for the sake of brevity). The hardening in all Cofalit-based foams was attributed to the precipitation of carbonate compounds, evidenced by the C-O stretching. Due to the 'noise' of intense diffraction lines (see the pattern for as received material in Fig. 8; a high crystallization degree may be understood from peaks neatly emerging from the background), we could not find confirmation from mineralogical analysis.

In all cases, the homogeneity of foams, before firing, was preserved after firing at 900 °C, as illustrated by Fig. 6b and e, showing a multitude of nearly spherical pores with a cell size well below 1 mm). The main differences between samples from different glass addition concerned the strength of the final products: as reported by Table 3, the compressive strength was acceptable, as ideally corresponding (applying the previously mentioned Gibson and Ashby model) to a solid phase with bending strength above 70 MPa (a reference value for soda lime glass) [6], only with 30 wt% SLG addition.

The addition of soda lime glass had a 'mineralizing' action, i.e. it did not simply offered a sintering aid, binding waste particles (Fig. 6c and f), as in the case of porcelain stoneware residue, but had a significant interaction, causing a modification of the phase assemblage. In the starting waste, an akermanite-based solid solution ($Ca_2Mg_{0.75}Al_{0.25}(Al_{0.25}Si_{1.75}O_7)$, PDF#79-2424) was clearly distinguishable as the main crystal phase, as reported by Fig. 8. The addition of SLG caused some 'glueing' of Cofalit particles, but also a change in the phase assemblage, which increased with increasing

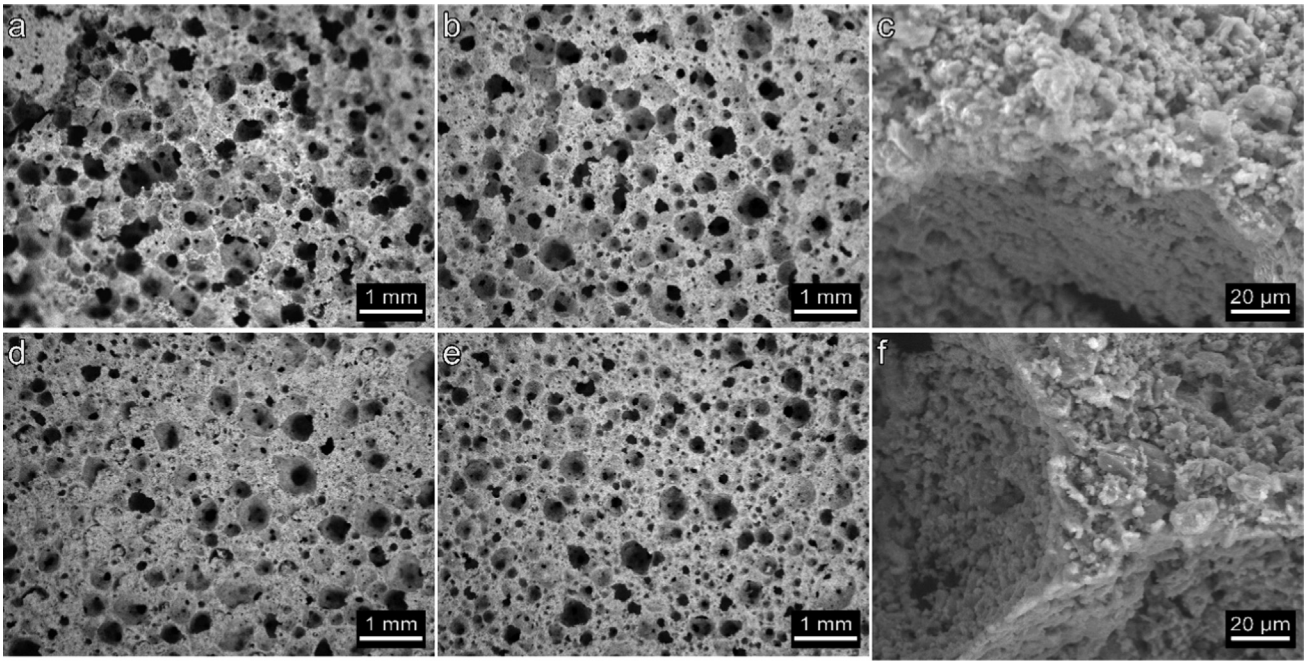

Fig. 6. Microstructural details of selected Cofalit-derived foams: a) C10SLG, 'green' foam; b-c) C10SLG, fired foam; d) C30SLG, 'green' foam; e-f) C30SLG, fired foam.

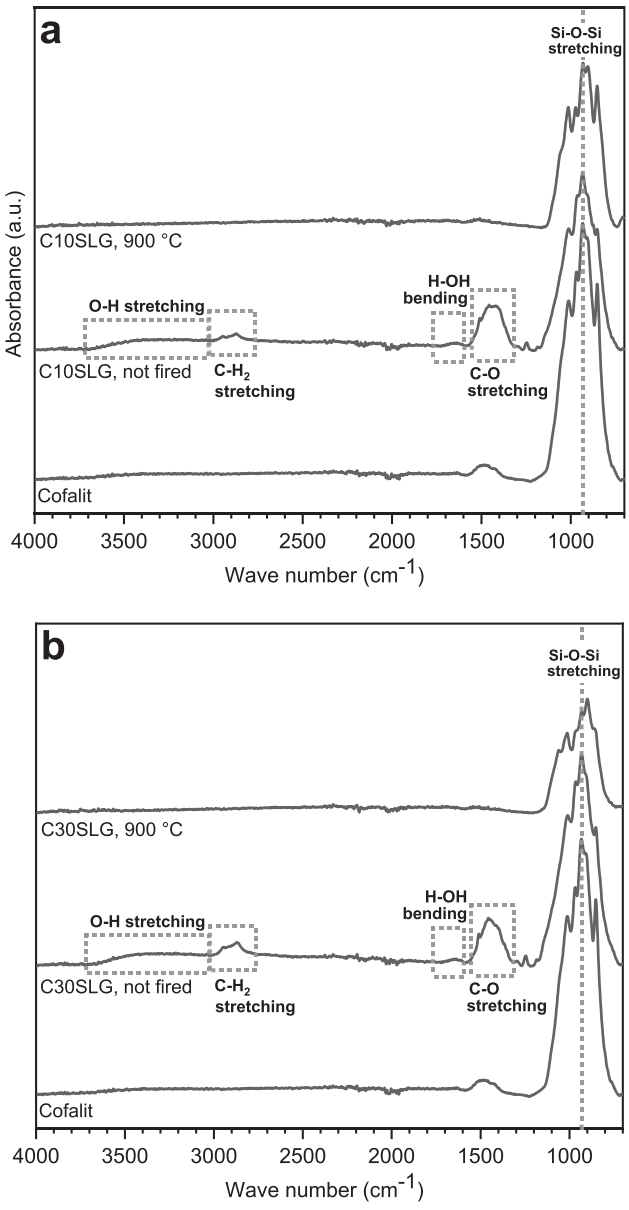

Fig. 7. FTIR analysis made on Cofalit and on C10SLG (a) and C30SLG (b) foams, before and after firing at 900 °C.

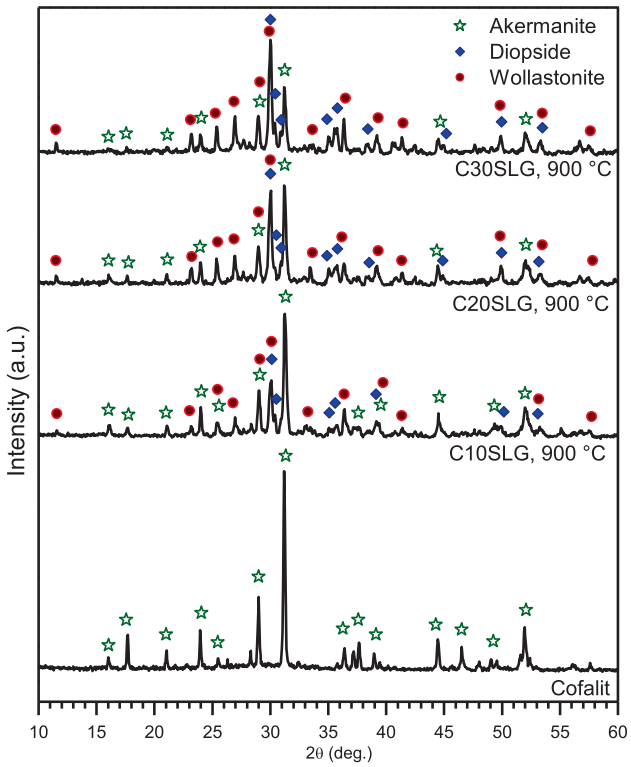

Fig. 8. XRD patterns of Cofalit and Cofalit-derived foams fired at 900 °C.

glass content. Diopside- and wollastonite-based solid solutions (Na-containing diopside, $(Ca_{0.91}Na_{0.05}Fe_{0.04})(Mg_{0.90}Fe_{0.07}Al_{0.03})(Si_{1.97}Al_{0.03})O_6$, PDF#80-1861, and Fe-containing wollastonite, $Ca_{2.87}Fe_{0.13}(SiO_3)_3$, PDF#83-2198, respectively) were promoted, whereas akermanite decreased. The glass addition, in other words, configured a condition of 'glass reactive sintering', according to which a vast range of glass-ceramics may come from reaction between softened glass and oxides (pure or combined, e.g. in silicates, termed as 'crystallization promoters') [29–32].

The phase evolution, with increasing glass additive, may be understood as an analogy with what occurring in glass-ceramics from the interaction of a silica-poor melilite (gehlenite, $Ca_2Al_2SiO_7$) with window glass (yielding wollastonite) [26], and, above all, in glass-ceramics from vitrified bottom ash. In the latter system, akermanite, developed at low sintering temperature, transformed into wollastonite and diopside by reaction with SiO_2 ($Ca_2MgSi_2O_7$ + $SiO_2 \rightarrow CaSiO_3 + CaMgSi_2O_6$) from the residual glass phase, at higher temperature [21]. In the present case, the extra silica could derive from the glass additive, and the reaction could be favoured by the fluxing action of alkali, both from the same SLG and from the activating solution. It is interesting to note that a 'competition' between melilite and pyroxene (families of solid solutions including akermanite and diopside, respectively) had been found also in the sinter-crystallization of remelted Cofalit [15], with pyroxene favored by the adoption of fast heating cycles, enhancing surface nucleation.

The much improved strength with 30 wt% soda-lime glass, corresponding to a decreased content of akermanite and an increased content of wollastonite, could be justified, in our opinion, by reduced internal stresses. Internal stresses could arise, upon cooling from the sintering temperature, from the significant mismatch in thermal expansion coefficient between crystal phase (supplied by Cofalit) and glass binding phase (supplied by SLG). In fact, akermanite exhibits a much larger thermal expansion coefficient ($\alpha > 30{\cdot}10^{-6}\ K^{-1}$) [33] than that of soda-lime glass ($\alpha \sim 9{\cdot}10^{-6}\ K^{-1}$) [34]. The promotion of silicate phase, like wollastonite, possessing a lower thermal expansion coefficient ($\alpha \sim 6.5{\cdot}10^{-6}\ K^{-1}$) [35], undoubtedly mitigated the mismatch.

4. Conclusions

We may conclude that:

- Highly porous materials could be easily obtained by alkali activation, gel-casting and sintering of partially crystallized residues, such waste from the polishing of porcelain stoneware or vitrified asbestos-containing waste;
- The gelation was caused by the formation of hydrated sodium carbonates, decomposed upon viscous flow sintering;
- The addition of soda-lime glass powders enabled the gelation of suspensions even operating at low molarity of NaOH activator; in the case of vitrified asbestos containing waste, a relatively

high glass addition was not necessary to promote gelation, but it had a fundamental impact on the phase development, by extensive interaction with the crystallized residue;
- Optimized conditions led, for both types of waste, to foams with high strength-to-density ratio; this was favored not only by the effectiveness of densification, but also by the engineering of crystal phases, with glass addition.

CRediT authorship contribution statement

P. Rabelo Monich: Software, Validation, Investigation, Conceptualization, Methodology, Formal analysis, Writing - original draft. **A. Rincon Romero:** Software, Validation, Investigation, Conceptualization, Methodology, Formal analysis, Writing - original draft. **E. Rambaldi:** Methodology, Formal analysis, Writing - original draft. **E. Bernardo:** Funding acquisition, Project administration, Supervision, Conceptualization, Methodology, Formal analysis, Writing - original draft.

Declaration of Competing Interest

The authors declare that they have no known competing financial interests or personal relationships that could have appeared to influence the work reported in this paper.

Acknowledgement

The research leading to these results has received funding from the European Union's Horizon 2020 research and innovation programme under the Marie Sklodowska-Curie grant agreements No. 721185 "NEW-MINE" (EU Training Network for Resource Recovery through Enhanced Landfill Mining; website: http://new-mine.eu/).

The authors would like to thank Dr. Erica Edme, Dr. Ulysse Michon and Dr. Nicolas Planty at Europlasma (Bordeaux, France) for supplying Cofalit ® vitrified waste, and Mr Federico Bottaro (University of Padova), for experimental assistance.

References

[1] B. Abu-Jdayil, A.H. Mourad, W. Hittini, M. Hassan, S. Hameedi, Traditional, state-of-the-art and renewable thermal building insulation materials: An overview, Constr. Build. Mater. 214 (2019) 709–735, https://doi.org/10.1016/j.conbuildmat.2019.04.102.
[2] G. Scarinci, G. Brusatin, E. Bernardo, Glass Foams, in: Cell. Ceram. Struct. Manuf. Prop. Appl., WILEY-VCH Verlag GmbH & Co. KGaA, Weinheim, 2005: pp. 158–176. doi:10.1002/3527606696.
[3] L. Ye, J. Hong, X. Ma, C. Qi, D. Yang, Life cycle environmental and economic assessment of ceramic tile production: A case study in China, J. Clean. Prod. 189 (2018) 432–441, https://doi.org/10.1016/j.jclepro.2018.04.112.
[4] http://uk.foamglas.com/__/frontend/handler/document.php?id=131&type=42 (accessed January 4, 2017).
[5] J. König, R.R. Petersen, Y. Yue, D. Suvorov, Gas-releasing reactions in foam-glass formation using carbon and Mn x O y as the foaming agents, Ceram. Int. 43 (2017) 4638–4646, https://doi.org/10.1016/j.ceramint.2016.12.133.
[6] A. Rincón, G. Giacomello, M. Pasetto, E. Bernardo, Novel 'inorganic gel casting' process for the manufacturing of glass foams, J. Eur. Ceram. Soc. 37 (2017) 2227–2234, https://doi.org/10.1016/j.jeurceramsoc.2017.01.012.
[7] H. Elsayed, A.R. Romero, L. Ferroni, C. Gardin, B. Zavan, E. Bernardo, Bioactive glass-ceramic scaffolds from novel "inorganic gel casting" and sinter-crystallization, Materials (Basel) 10 (2017), https://doi.org/10.3390/ma10020171.
[8] A.R. Romero, S. Tamburini, G. Taveri, J. Toušek, I. Dlouhy, E. Bernardo, Extension of the "inorganic gel casting" process to the manufacturing of boro-aluminosilicate glass foams, Materials (Basel) 11 (2018) 1–12, https://doi.org/10.3390/ma11122545.
[9] Confindustria Ceramica, Italian Integrated Report, 2019.
[10] F. Andreola, L. Barbieri, I. Lancellotti, C. Leonelli, T. Manfredini, Recycling of industrial wastes in ceramic manufacturing: State of art and glass case studies, Ceram. Int. 42 (2016) 13333–13338, https://doi.org/10.1016/j.ceramint.2016.05.205.
[11] E. Rambaldi, L. Esposito, A. Tucci, G. Timellini, Recycling of polishing porcelain stoneware residues in ceramic tiles, J. Eur. Ceram. Soc. 27 (2007) 3509–3515, https://doi.org/10.1016/j.jeurceramsoc.2007.01.021.
[12] G.A. Ramos, F. Pelisser, P.J. Paul Gleize, A.M. Bernardin, M.D. Michel, Effect of porcelain tile polishing residue on geopolymer cement, J. Clean. Prod. 191 (2018) 297–303, https://doi.org/10.1016/j.jclepro.2018.04.236.
[13] Inertam-Europlasma, Asbestos processing and recycling. http://www.inertam.com/le-traitement-de-lamiante-sa-valorisation/?lang=en (accessed August 10, 2019).
[14] D. Spasiano, F. Pirozzi, Treatments of asbestos containing wastes, J. Environ. Manage. 204 (2017) 82–91, https://doi.org/10.1016/j.jenvman.2017.08.038.
[15] E. Bernardo, L. Esposito, E. Rambaldi, A. Tucci, Sintered glass ceramic articles from plasma vitrified asbestos containing waste, Adv. Appl. Ceram. 110 (2011) 346–352, https://doi.org/10.1179/1743676111y.0000000020.
[16] I. Garcia-Lodeiro, A. Fernández-Jimenez, P. Pena, A. Palomo, Alkaline activation of synthetic aluminosilicate glass, Ceram. Int. 40 (2014) 5547–5558, https://doi.org/10.1016/j.ceramint.2013.10.146.
[17] P.R. Monich, A.R. Romero, D. Höllen, E. Bernardo, Porous glass-ceramics from alkali activation and sinter-crystallization of mixtures of waste glass and residues from plasma processing of municipal solid waste, J. Clean. Prod. 188 (2018) 871–878, https://doi.org/10.1016/j.jclepro.2018.03.167.
[18] E. Bernardo, L. Esposito, E. Rambaldi, A. Tucci, Y. Pontikes, G.N. Angelopoulos, Sintered esseneite-wollastonite-plagioclase glass-ceramics from vitrified waste, J. Eur. Ceram. Soc. 29 (2009) 2921–2927, https://doi.org/10.1016/j.jeurceramsoc.2009.05.017.
[19] M. Dondi, G. Ercolani, C. Melandri, C. Mingazzini, M. Marsigli, The chemical composition of porcelain stoneware tiles and its influence on microstructural and mechanical properties, Int. Ceram. Rev. 48 (1999).
[20] J. Martín-Márquez, A.G. De la Torre, M.A.G. Aranda, J.M. Rincón, M. Romero, Evolution with temperature of crystalline and amorphous phases in porcelain stoneware, J. Am. Ceram. Soc. 92 (2009) 229–234, https://doi.org/10.1111/j.1551-2916.2008.02862.x.
[21] A. Rincon Romero, M. Salvo, E. Bernardo, Up-cycling of vitrified bottom ash from MSWI into glass-ceramic foams by means of 'inorganic gel casting' and sinter-crystallization, Constr. Build. Mater. 192 (2018) 133–140, https://doi.org/10.1016/j.conbuildmat.2018.10.135.
[22] P. Rabelo Monich, F. Dogrul, H. Lucas, B. Friedrich, E. Bernardo, Strong porous glass-ceramics from alkali activation and sinter-crystallization of vitrified MSWI bottom ash, Detritus. Volume 08 (2019) 1. doi:10.31025/2611-4135/2019.13881.
[23] G. Biffi, R. Giovannini, Book for the production of the ceramic tiles, Gruppo Editoriale Faenza, Faenza, 2003.
[24] L.K. Kazantseva, T.Z. Lygina, S.V. Rashchenko, D.S. Tsyplakov, Preparation of sound-insulating lightweight ceramics from aluminosilicate rocks with high $CaCO_3$ content, J. Am. Ceram. Soc. 98 (2015) 2047–2051, https://doi.org/10.1111/jace.13581.
[25] L.J. Gibson, M.F. Ashby, Cellular solids: structure and properties, Cambridge University Press, Cambridge, UK, 1999.
[26] A. Rincón, M. Marangoni, S. Cetin, E. Bernardo, Recycling of inorganic waste in monolithic and cellular glass-based materials for structural and functional applications, J. Chem. Technol. Biotechnol. 91 (2016) 1946–1961, https://doi.org/10.1002/jctb.4982.
[27] W.A. Deer, R.A. Howie, W.S. Wise, J. Zussman, Rock-Forming Minerals, Vol. 4B. Framework Silicates: Silica Minerals, Feldspathoids and the Zeolites, 2nd ed., The Geological Society, London, 2004. https://books.google.it/books?id=c4H5TsJbUdsC.
[28] J. Marcial, J. Kabel, M. Saleh, N. Washton, Y. Shaharyar, A. Goel, et al., Structural dependence of crystallization in glasses along the nepheline (NaAlSiO4) – eucryptite (LiAlSiO4) join, J. Am. Ceram. Soc. 101 (2018) 2840–2855, https://doi.org/10.1111/jace.15439.
[29] R. Müller, R. Meszaros, B. Peplinski, S. Reinsch, M. Eberstein, W.A. Schiller, et al., Dissolution of alumina, sintering, and crystallization in glass ceramic composites for LTCC, J. Am. Ceram. Soc. 92 (2009) 1703–1708, https://doi.org/10.1111/j.1551-2916.2009.03089.x.
[30] W. Zhang, H. Liu, A low cost route for fabrication of wollastonite glass–ceramics directly using soda-lime waste glass by reactive crystallization–sintering, Ceram. Int. 39 (2013) 1943–1949, https://doi.org/10.1016/j.ceramint.2012.08.044.
[31] W. Si, C. Ding, An investigation on crystallization property, thermodynamics and kinetics of wollastonite glass ceramics, J. Cent. South Univ. 25 (2018) 1888–1894, https://doi.org/10.1007/s11771-018-3878-5.
[32] W. Si, Z.Y. Wang, W.Y. Zhang, W. Pan, Preparation of glass-ceramics by reactive crystallization with waste glass and mullite, Key Eng. Mater. 697 (2016) 561–564, https://doi.org/10.4028/www.scientific.net/KEM.697.561.
[33] M. Merlini, M. Gemmi, G. Artioli, Thermal expansion and phase transitions in åkermanite and gehlenite, Phys. Chem. Miner. 32 (2005) 189–196, https://doi.org/10.1007/s00269-005-0458-7.
[34] K. Yamamoto, N. Hasaka, H. Morita, E. Ohmura, Influence of thermal expansion coefficient in laser scribing of glass, Precis. Eng. 34 (2010) 70–75, https://doi.org/10.1016/j.precisioneng.2009.03.005.
[35] Physical Properties of Wollastonite. http://imerys-additivesformetallurgy.com/wp-content/uploads/Physical-Properties-Overview.pdf (accessed March 23, 2020).